Superlattices and Microstructures 90 (2016) 45–52

Contents lists available at ScienceDirect

Superlattices and Microstructures

journal homepage: www.elsevier.com/locate/superlattices

Structural, morphological and optical properties of ZnO nano-fibers

K. Thangavel [a], A. Balamurugan [b], T. Venkatachalam [c], E. Ranjith Kumar [d, *]

[a] Department of Electronics, SNR Sons College, Coimbatore, 641006, India
[b] Department of Physics, Government Arts College, Udhagamandalam, 643002, India
[c] Department of Physics, Coimbatore Institute of Technology, Coimbatore, 641014, India
[d] Department of Physics, Dr. NGP Institute of Technology, Coimbatore, 641048, India

ARTICLE INFO

Article history:
Received 27 November 2015
Received in revised form 7 December 2015
Accepted 10 December 2015
Available online 13 December 2015

Keywords:
Electro-spin coating
Nano-fibers
ZnO

ABSTRACT

Microcontroller aided electro-spin coating unit was designed and optimized to fabricate nano-fibers. Composite nano-fibers of ZnO were fabricated using this unit. The ZnO fibers were annealed at different temperatures from 200 °C to 600 °C using muffle furnace, all the continuous fibers were found to be defect free and beads free. The structural and composition of the fibers are analyzed using XRD and EDAX measurements. The X-ray diffraction peaks revealed that the fibers are wurtzite hexagonal structure. The composition of the fiber is confirmed as ZnO from the percentage of constituents of Zinc and Oxygen in EADX results. The optical properties of the fibers are studied by using spectrophotometer. The optical band gap energy is found to be 3.37 eV. The surface morphology of the fiber was studied using SEM and TEM analysis. The fibers are found to be defect free and they are excellent material for high sensitive optoelectronic sensors.

1. Introduction

Nowadays optoelectronic devices play vital role in this modern medical field. The materials of optoelectronic devices should have excellent physical and chemical properties and also inexpensive and biodegradable in nature. Nano-fibers of zinc oxide (ZnO) materials plays a dynamic role in fabricating light emitting diodes, photo detectors and solar cells and also it is used as substitute material for Si and Ge in optoelectronic devices [1–4]. ZnO is a biodegradable semiconducting material with band gap energy of 3.37 eV and excitation binding energy of 60 meV at room temperature [5,6]. ZnO thin films have an exceptional blend of interesting properties such as electrical, optical and excellent substrate adherence, hardness and piezo electric behaviors [7,8].

All the conventional preparation techniques of nano-fibers have a multitude of difficulties including long or complex procedures for preparation, high processing temperatures and residual organic solvent in the final polymer [9]. In addition, the control over pore size and interconnectivity are unsatisfactory that is the size of the base polymer and the pore vary from few micrometer to hundreds of micrometers. The electro-spin coating technique can avoid these difficulties and achieves self-assembly, phase separation, force spinning and flash spinning. This technology has numerous advantages like easily controllable, able to generate continuous fibers and especially to fabricate nano-fibers with diameters in the nanometer size

* Corresponding author.
E-mail addresses: kthangavel@yahoo.co.in (K. Thangavel), ranjueaswar@gmail.com (E. Ranjith Kumar).

http://dx.doi.org/10.1016/j.spmi.2015.12.004
0749-6036/

[10,11]. Newly introduced programed microcontroller electro-spin coating unit has made the cost effective, portable and allow us to control the voltage preciously during the fabrication of fibers in this research and this is the pioneer in nano-technology. These motivated us to choose microcontroller interfaced electrospinning technology for the preparation of ZnO nano-fibers in this research.

2. Experimental details

2.1. Fabrication of microcontroller aided electro-spin coating unit

The microcontroller aided electro-spin coating unit is designed and constructed as shown in the schematic diagram Fig. 1. The system consists of three major units: i) variable power supply unit (0–30 kV), ii) spinneret-solution feeding unit and iii) nano-fiber collecting unit. The power supply unit which is connected to the tip of the syringe and the collecting unit is essential part in electro-spin technique to produce very high voltage (up to 30 kV) and to spawn the nano-fibers.

Spinneret-solution feeding unit is made up of syringe (with stainless steel needle of size 0.1 mm-0.3 mm) fitted with syringe holder and connected to the stepper motor. The stepper motor is used to generate the precise amount of forward and reverse mechanical force to move the piston of the syringe forward and backward using microcontroller unit and have Taylor cone formed, followed by aligned nano-fibers are fabricated as the substrate (fitted in the metal collector holder) The high voltage power supply unit is used to generate 30 kV DC between the needle and collecting unit. During forward motion the Sol-Gel comes out of the syringe needle tip.

2.2. Fabrication of ZnO nano fibers

2.2.1. Preparation of precursor solution

3 g purity tested (99% Sigma Aldrich) PVA, and 6 g Zinc acetate dihydrate (99% Merck) were dissolved with 40 ml triple distilled water in two separate beakers, and then the solutions were mixed in different ratios 1:1, 1:2 and 1:3 in separate beakers using magnetic stirrer for three hours at room temperature. The mixtures were stored for 24 h aging period at room temperature to form high viscous state for this sol–gel technique [12]. The prepared precursor solution was sucked without any air bubbles in the syringe. The syringe was fitted in the syringe holder setup and aligned to be in the same horizontal axis with shaft of the stepper motor.

2.2.2. Preparation of glass substrates

Glass substrates of size 2.5 × 37.5 sq mm were cleaned by the following process. i) the glass substrates were soaked in Sodium hydroxide solution for 25 min to remove grease and fat substances, ii) cleaned using detergent solution and running distilled water, iii) cleaned using ultrasonic agitator for 30 min in distilled water mixed with few drops of detergent solution to remove residues, iv) cleaned with pure Isopropanol for vapor degreasing and then transferred to a beaker containing distilled water and to the beaker containing acetone and v) the cleaned substrates were kept in oven for an hour at 423 K. Finally the well cleaned substrates were stored in the vacuum desiccators.

2.2.3. Optimization of electro-spin coating unit

Microcontroller (PIC 16F877A) fitted board was connected with computer and codes written in 'C 'language to operate the stepper motor were flashed (stored). The operating voltage was drawn from the 6 V DC power supply unit. Using test solution (appropriate viscous sugar solution) in syringe the expected movement of the piston and flow of liquid from the tip of the

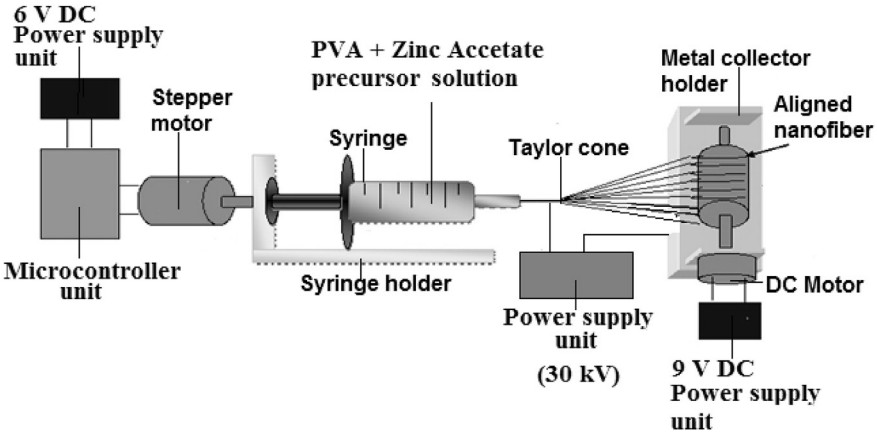

Fig. 1. Schematic diagram of electro-spin coating unit.

stainless steel needle was assured. Another similar programmed microcontroller fitted board, and inverter (with potentiometer) were attached along the line output transformer (LOT) and the output terminals were connected across the needle of the syringe and substrate fitted metal holder to apply high voltage. The expected variation of voltage across needle and the holder from 1 kV to 30 kV with adjustment of the potentiometer was measured and the potentiometer was calibrated.

2.2.4. Preparation of ZnO nano-fibers

The high voltage applied between the needle and metal holder was used to heat the precursor solution and to form the tailor cone at the tip of the needle without decomposition of polyvinyl alcohol (PVA) and Zinc acetate dihydrate. Due to the forward movement of piston and applied high voltage, the tailor cone was formed and made as nano fiber. The composite nano fibers of PVA and Zinc acetate dihydrate were spawned on the cleaned glass substrate (mounted on collector holder). The nano-fibers deposited glass substrates were collected labeled and preserved in desiccators then and there. All the deposited films were inspected to have good properties with the help of XRD, SEM and FESEM analysis. The optimal data of the chemical compositions and parameters are tabulated as shown in Table 1.

3. Results and discussion

3.1. Structural properties of ZnO nano fibers

The XRD spectra of ZnO nano fibers (annealed at three temperatures are 400 °C, 500 °C, 600 °C) as shown in Fig. 2. Prominent peaks are found at (2θ) 31.3°, 34°, 35.8° 47.1°, 56.2°, 62.5°, and 67.6° in all the ZnO nano fibers. The predominant peaks in XRD graph of ZnO nano fibers could be probably associated with (100), (002), (101), (102), (110), (103) and (112) reflections of the wurtzite hexagonal structure respectively (JCPDS card 36–1451) [13].

The lattice constants "a" and "c" were calculated for the ZnO from the high intensity peaks using the relation (1) and the lattice constants were found to be nearly 3.27 Å (a), and 5.27 Å (c).

$$\frac{1}{d^2} = \frac{4}{3}\frac{h^2 + hk + k^2}{a^2} + \frac{l^2}{c^2} \tag{1}$$

Where d is the lattice spacing h, k, l are miller indices.

The average crystallite size of the wurtzite phase was estimated from the high intensity peak in the XRD patterns using Scherrer formula (2) [14].

$$D = \frac{0.9\,\lambda}{\beta \mathrm{Cos}\theta} \tag{2}$$

Where "λ" is the wavelength of X-rays, "β" is the full width at half maximum (FWHM) of the high intensity peak and θ is the Bragg's angle of the radians. The strain (ε) was calculated from the slope of β cos θ versus sin θ plot using the relation (3).

$$\beta = \frac{\lambda}{D\ \mathrm{Cos}\ \theta} - \varepsilon\ \tan\ \theta \tag{3}$$

The dislocation density was determined from the relation (4).

$$\delta = \frac{1}{D^2} \tag{4}$$

The lattice parameters, particle sizes, strain, and dislocation densities of thin films deposited are tabulated as shown in Table 2.

The composition of the films was estimated by EDAX measurement and it is found to be 78.85% and 21.15% for Zn and O elements respectively. The EDAX spectrum is shown in Fig. 3. The molecular formula of the compound was identified as ZnO.

Table 1
Range of parameters and optimized data for ZnO nano fibers depositions.

S. no	Parameter	Range	Optimized data
1	Tip of the needle to substrate	7 cm to 22 cm	15 cm
2	Applied high voltage across needle and substrate	15 kV–20 kV	17 kV
3	Needle diameter	0.1 mm–1 mm	0.1 mm–0.3 mm
4	Ratio of PVA to zinc acetate dihydrate	1:1, 1:2, 1:3	1:2
5	Annealing temperature	200 °C–600 °C	600 °C

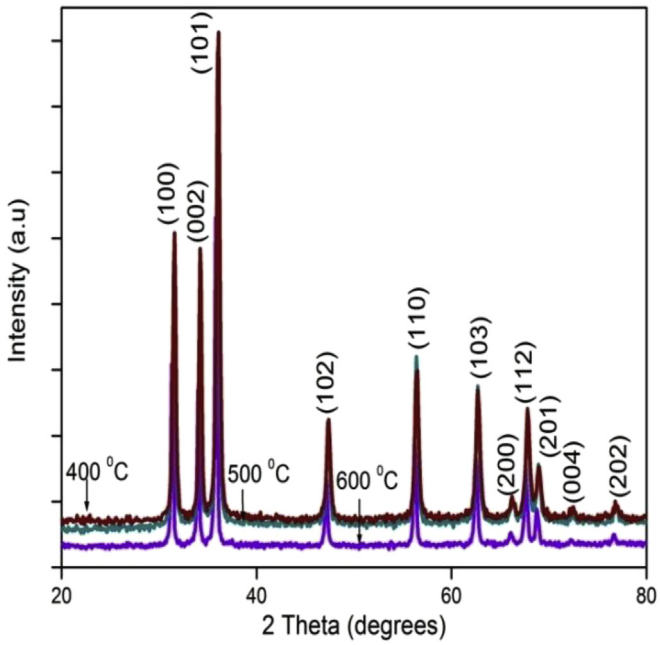

Fig. 2. XRD spectra of ZnO nano fibers deposited on glass substrate.

Table 2
The values of crystal size, lattice constant, strain, and stress and dislocation density for XRD peaks.

Annealed temperature (° C)	Miller indices			Crystal size (nm)	Lattice constant (D)		Strain ($\times 10^{-4}$ lines^{-2} m^4)	Dis-location density (δ) ($\times 10^{-4}$ lines^{-2} m^2)
	h	K	l		a (Å)	c (Å)		
400	1	0	1	21.90	3.27	5.23	0.0013	1.12
	1	0	0	22.15			0.0015	1.36
	0	0	2	23.47			0.0011	1.42
500	1	0	1	24.95	3.27	5.24	0.0012	1.60
	1	0	0	24.82			0.0013	1.62
	0	0	2	25.42			0.0010	1.54
600	1	0	1	29.15	3.27	5.27	0.0010	1.76
	1	0	0	28.14			0.0012	1.26
	0	0	2	29.86			0.0009	1.12

3.2. Surface morphology of ZnO nano fibers

The surface morphology and size of the fabricated nano-fibers were evaluated by Field Emission Scanning Electron Microscopy (FESEM) (FEI-QUANTA-FEG250) with 1.0 nm resolution and 30 kV operating voltage [15]. High Resolution Transmission Electron Microscopy (HRTEM) JEOL JEM 2100 Model with lattice resolution of 0.14 nm and point - to – point resolution of 0.19 nm [16]. The electro-spin nano-fibers diameter and morphology were studied on various inputs and processing parameters such as: voltage applied, distance between needle and collector, polymer type, solution viscosity, surface tension, and feeding rate [17]. The best nano-fibers were obtained on the above quoted optimum values in Table 1. Figs. 4 and 5 denote FESEM and TEM images of a) PVA/Zinc acetate composite nano-fibers and b) ZnO nano-fibers. In addition, humidity and temperatures of the production environment also affects the nano-fibers [18]. It clearly shows that the composite nano-fibers have smooth surfaces and diameters that vary from 10 nm to 500 nm. It is also observed from the results that the annealed ZnO nano-fibers diameters are smaller than unannealed nano-fibers. These result exhibits excellent characteristics, such as large surface area per unit mass [19] (for example nearly 100 nm fiber diameter have specific surface of nearly 1000 m^2/g), coupled with remarkable porosity, and outstanding mechanical, structural, and axial strength. These fabricated fibers have unique characteristics, such as diameters that start from 10 nm long, and will play a significant role in optoelectronics devices [20]. The thickness of the thin film was measured as the maximum diameter of the fiber in the FESEM image (500 nm).

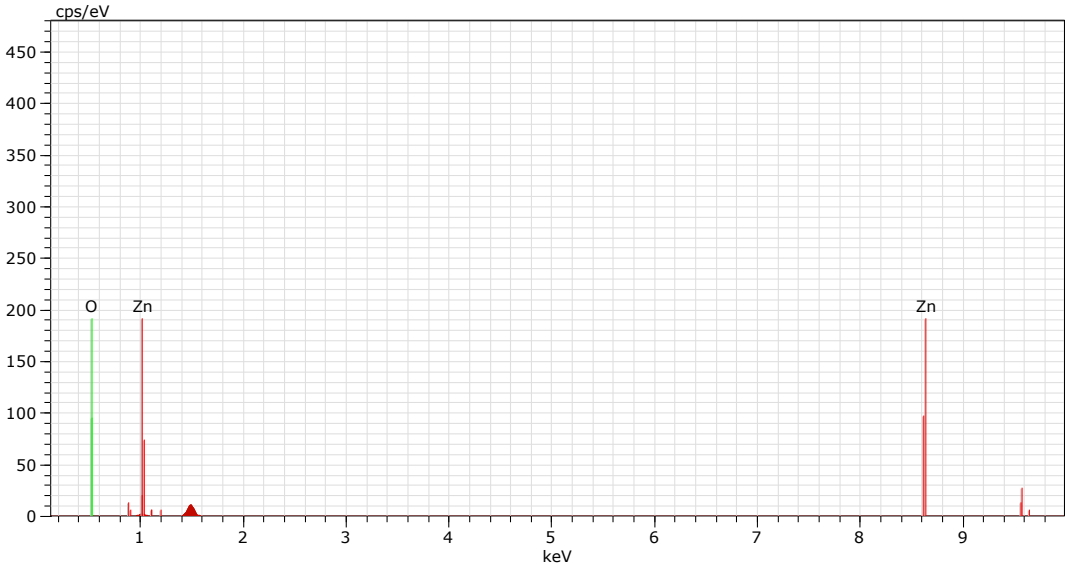

Fig. 3. EDAX spectrum for ZnO nano thin films.

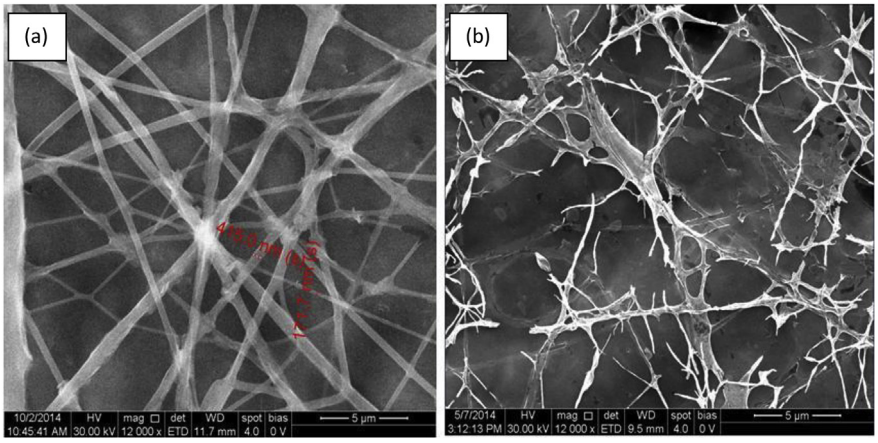

Fig. 4. FESEM images of a) PVA and zinc acetate dihydrate nano fibers b) ZnO nano-fibers deposited on glass substrate.

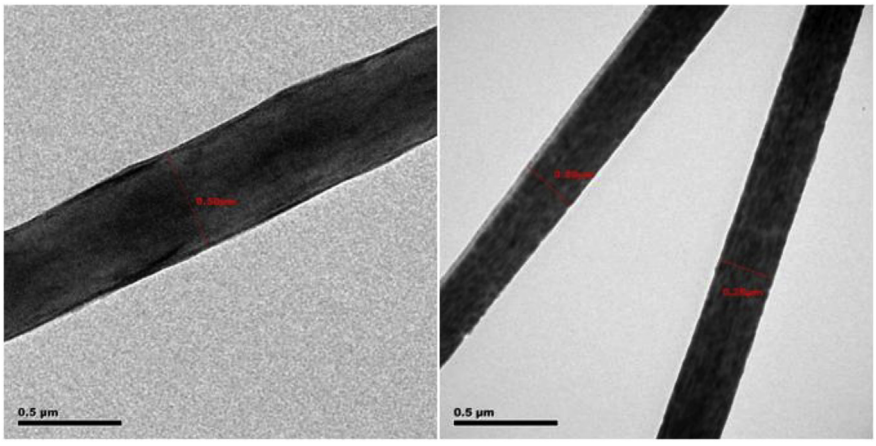

Fig. 5. TEM images of PVA and zinc acetate dihydrate nano fibers.

3.3. Thermal properties of ZnO nano fibers

The thermal stability of the fabricated PVA/Zinc acetate dihydrate nano fibers was investigated using thermogravimetric analysis from 25 °C to 600 °C (Simultaneous thermal analyzer (Thermo-gravimetric & Differential scanning calorimetry) TGDSC). Fig. 6 defines the thermal activities of the generated nano-fibers. There are three significant weight losses occurring in the thermogravimetric (TG) characteristics curve. The first weight loss is almost 22% in the range of 40 °C–120 °C. This specific weight loss is due to the loss of the residual water molecules or surface absorbed water in the precursor composite fibers. The first endothermic peak appeared around 105 C in the Differential Scanning Calorimeter (DSC) curve which is described by Fig. 6. This was detected due to the decomposition of the acetate group and evaporation of water. It is reported that standard crystallization starts around 250 °C [21]. The second weight loss is around 33% in the range of 200 °C–303 °C, caused by the loss of the volatile components, including H_2O, CO, and CO_2.

The third weight loss is nearly 20% in the TG curve, occurring from 303 °C to 480 °C. This weight loss corresponds to the decomposition of the PVA. The exothermic peaks absorbed around 255 °C, 285 °C and 500 °C in the DSC curve can be attributed to the vaporization of the acetate side chain and the main chain of PVA [22]. The decomposition of the PVA/zinc becomes constant beyond 480 °C. A thermal analysis result very clearly clarifies that no weight loss occurs after 480 °C.

3.4. UV–Visible studies of ZnO nano fibers

Optical absorption and transmission spectra of composite nano-fibers and fibers which are annealed at 400 °C, 500 °C and 600 °C are shown in Figs. 7 and 8. The UV absorption edge of the ZnO nano-fibers were recorded in the wavelength range from 250 nm to 1400 nm. The spectra results expose that the absorption edge of ZnO nano-fibers varied from 3.40 eV to 3.35 eV. With this result, the annealing at 400 °C has its maximum bandwidth, and annealing at 600 °C has its minimum bandwidth. These results clearly show that band gap energy is closely associated with annealing temperatures.

Fig. 7(a) and (b) represents PVA/Zinc acetate composite nano-fibers the results show significantly larger band gaps compared to the annealed one. The larger value of the band gap can be attributed to the presence of PVA and other molecules such as unreacted solvents. Many research experts state that the crystal structure of ZnO annealing temperatures begins at 200 °C or higher. The band gap, refractive index (ν) and Extinction coefficient (k) values were calculated and its values are tabulated in Table 2.

The high intensity spectra peaks were used to calculate the optical band gap, using the relation (5).

$$(\alpha h\nu)^n = A\,(h\nu - E_g) \tag{5}$$

Where hν is the photon energy, A denotes proportionality constant and exponent n depends on the type of optical transition which is ½ for all allowed direct transition. The extinction coefficient (k) is calculated by the following relation.

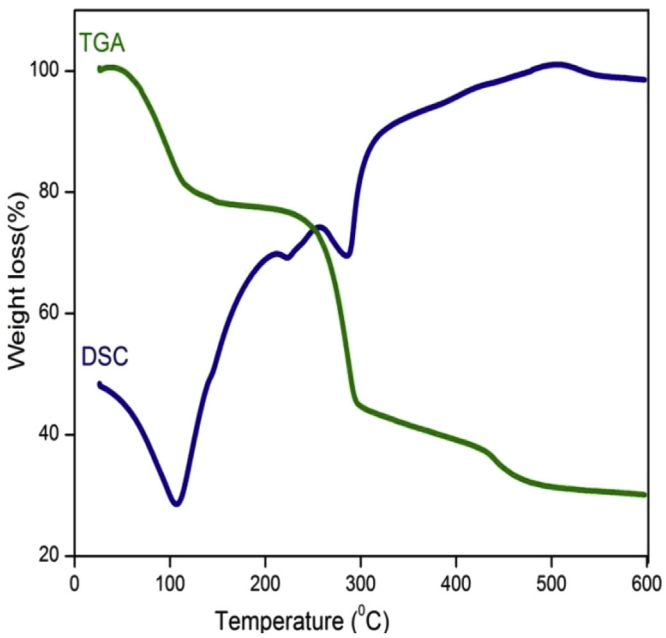

Fig. 6. TGA and DSC graphs of PVA and Zinc acetate dihydrate nano fibers.

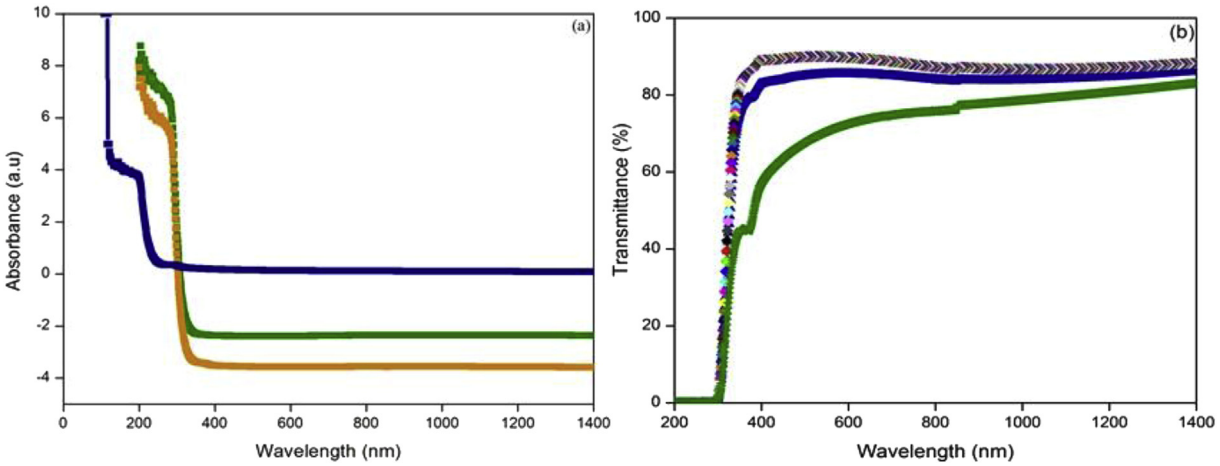

Fig. 7. Absorbance and transmittance graphs of PVA and Zinc acetate dihydrate nano fibers by UV–Visible studies.

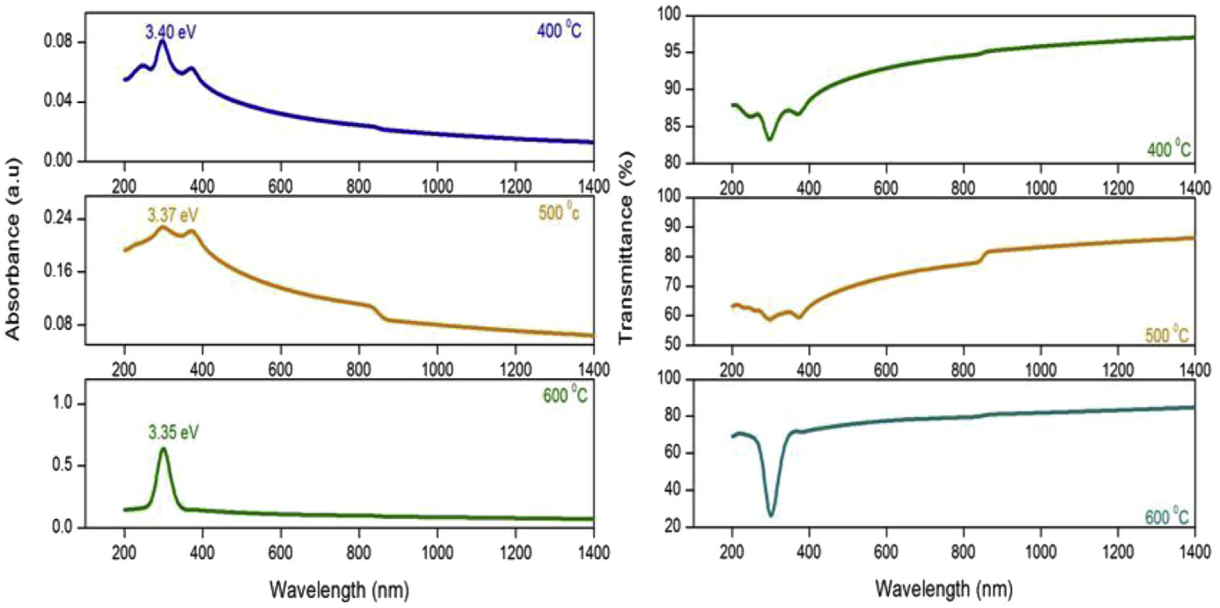

Fig. 8. Absorbance and transmittance graphs of ZnO nano fibers by UV–Visible studies at 400 °C, 500 °C and 600 °C.

$$K = \alpha\lambda / 4\pi \tag{6}$$

The refractive index of the nano-fibers sample (n) is determined using the relation (7).

$$t = [n + (n_2 - n_0 \cdot n_1)^{1/2}]^{1/2} \tag{7}$$

Where t is the thickness of the film, n_0 is the refractive index of the air and n_1 is the refractive index of the glass substrate.

The variation of direct band gap with annealing temperature is shown in Table 3. It shows that when annealing temperatures increase, the band gap consequently decreases [23]. In addition, all spectra reports clearly prove that the fabricated nano-fibers have excellent structure, refractive index, and extinction coefficient. These results state that this kind of material can be considered for photo catalytic, optoelectronics, and light emitting applications [24].

Table 3
UV–Vis optical properties of PVA/zinc acetate nano-fibers.

Annealed temperature	Band gap (E_g eV)	Extension co-efficient (K)	Refractive index (v)
400° C	3.40	0.0185	1.96
500° C	3.37	0.0187	1.97
600° C	3.35	0.0188	1.98

4. Conclusion

Nano-fibers of ZnO were fabricated by the newly developed electro-spin coating unit. The effect of structure, surface morphology, and optical properties of ZnO nano-fibers were systematically investigated. The average diameter of the fabricated nano-fibers is 25.53 nm. Structural analysis results clearly show that the fabricated nano-fibers were identified with phase of wurtzite hexagonal structure. The crystal size increases from 21.79 nm to 29.86 nm with increasing annealing temperature and at the same time the stress and strains are reduced from 0.0013 to 0.0009 and 0.0069 to 0.0050 respectively. The band gaps of annealed and unannealed fabricated fibers were calculated from optical spectra. Based on these results, we strongly believe that the fabricated nano-fibers with excellent optical property, could be used for the fabrication of opto-electronic nano-devices.

References

[1] Zhong Lin Wang, J. Phys. Condens. Matter 16 (2004) R829–R858.
[2] Alberto Adan-Mas, Di Wei, Nanomaterials 3 (2013) 325–356.
[3] J.H. Na, M. Kitamura, M. Arita, Y. Arakawa, Appl. Phys. Lett. 95 (25) (2009) 12–21.
[4] P. Sudhagar, R.S. Kumar, J.H. Jung, W. Cho, R. Sathyamoorthy, J. Won, Mater. Res. Bull. 46 (9) (2011) 1473–1479.
[5] Shahid Hussain, Tianmo Liu, M. Kashif, Liyang Lin, Shufang Wu, Weiwei Guo, Wen Zeng, U. Hashim, Mater. Sci. Semicond. Process. 18 (2014) 52–58.
[6] A. Satyanarayana Reddy, Yi-Hao Kuo, Shashi B. Atla, Chien Yen Chen1, Chien-Cheng Chen, Ruey-Chyuan Shih, Young-Fo Chang, Jyoti Prakash Maity, How-Ji Chen, J. Nano Sci. NanoTechnol. 11 (6) (2011) 5034–5041. J. Nucl. Sci. Technol.
[7] T. Ivanova, A. Harizanova, T. Koutzarova, B. Vertruyenc, J. Non-Cryst. Solids 357 (15) (2011) 2840–2845.
[8] V.R. Shinde, T.P. Gujar, C.D. Lokhande, Sol. Energy Mater. Sol. Cells 91 (2007) 1055–1061.
[9] Jing Tao, Effects of Molecular Weight and Solution Concentration on Electrospinning of PVA, a Thesis, Worcester Polytechnic Institute, 2003.
[10] Ioannis S. Chronakis, J. Mater. Process. Technol. 167 (2–3) (2005) 283–293.
[11] S.K. Nataraj, B.H. Kim, J.H. Yun, D.H. Lee, T.M. Aminabhavi, K.S. Yang, Carb. Lett. 9 (2) (2008) 108–114.
[12] Gibin George, S. Anandhan, Mater. Sci. Semicond. Process. 32 (2015) 40–48.
[13] Qu Zhou, Weigen Chen, Lingna Xu, Shudi Peng, Sensors 13 (2013) 6171–6182.
[14] N. Sadananda Kumar, Kasturi, V. Bangera, G.K. Shivakumar, Appl. Nanosci. 4 (2014) 209–216.
[15] Jeong-Ha Baek, Juyun Park, Jisoo Kang, Don Kim, Sung-Wi Koh, Yong-Cheol Kang, Bull. Korean Chem. Soc. 33 (8) (2012) 2694–2698.
[16] Yingjie Liao, Takeshi Fukuda, Norihiko Kamata, Makoto Tokunaga, Nanosci. Res. Lett. 9 (1) (2014) 267.
[17] C.J. Thompson, G.G. Chase, A.L. Yarin, D.H. Reneker, Polymer 48 (2007) 6913–6922.
[18] Maria S. Peresin, Youssef Habibi, Arja-Helena Vesterinen, Orlando J. Rojas, Joel J. Pawlak, Jukka V. Seppa, Biomacromolecules 11 (9) (2010) 2471–2477.
[19] T. Jeevani, J. Nanomed. Nanotechnol. 2 (2011) 124.
[20] W.U. Hui, P.A.N. Wei, L.I.N. Dandan, L.I. Heping, J. Adv. Ceram. 1 (1) (2012) 2–23.
[21] Ibrahim Uslu, Burcu Başer, Ahmet Yayli, Mehmet Levent Aksu, e-Polymers 7 (1) (2007) 1699–1704.
[22] S. El-Sayed, K.H. Mahmoud, A.A. Fatah, A. Hassen, Phys. B Condens. Matter 406 (21) (2011) 4068–4076.
[23] M.R. Islam, J. Podder, Cryst. Res. Technol. 44 (3) (2009) 286–292.
[24] J.H. Na, M. Kitamura, M. Arita, Y. Arakawa, Appl. Phys. Lett. 95 (25) (2009) 10452–10458.